Mathematical Models and Methods in Applied Sciences
Vol. 10, No. 2 (2000) 187–202

BLOOD FLOW THROUGH A CIRCULAR PIPE WITH AN IMPULSIVE PRESSURE GRADIENT

GIUSEPPE PONTRELLI*
Istituto per le Applicazioni del Calcolo, CNR,
Viale del Policlinico 137, 00161 Roma, Italy

Communicated by K. R. Rajagopal
Received 15 October 1998

The unsteady flow of a viscoelastic fluid in a straight, long, rigid pipe, driven by a suddenly imposed pressure gradient is studied. The used model is the Oldroyd-B fluid modified with the use of a nonconstant viscosity, which includes the effect of the shear-thinning of many fluids. The main application considered is in blood flow.

Two coupled nonlinear equations are solved by a spectral collocation method in space and the implicit trapezoidal finite difference method in time. The presented results show the role of the non-Newtonian terms in unsteady phenomena.

1. Introduction

Industrial and biological flows in pipes are quite common and have relevant applications. Since unsteadiness dominates most of such processes, flows due to the sudden variation of the pressure gradient are worth being studied, because they are the basis for understanding the material properties and the characteristics of other unsteady complex flows.

In the context of the linear Navier–Stokes theory, the basic problem was first solved by Szymanski.[28] The analytical solution can be found as superimposition of the Poiseuille flow and an unsteady solution expressed as combination of Bessel functions.

On the other hand, many recent studies pointed out the importance of non-Newtonian characteristics of many fluid materials both in technology and in nature. Marked viscoelastic properties possess fluids such as diluted polymers or suspensions, where a solid constituent is dissolved in a solvent. A variety of non-Newtonian models have been developed in the last years, as an expression of the rheological properties of many fluids.[4]

*E-mail: pontrelli@iac.rm.cnr.it

In Ref. 30, Ting analyzed the flow of an impulsive pressure gradient for a second order fluid in a circular tube. In his work, bounded solutions for physically acceptable values of the parameters cannot be found.

Etter and Schowalter studied the problem for the class of Oldroyd fluids, both in a step change in pressure and in a sinusoidally varying pressure gradient. They showed how the solution can overshoot the final steady state value.[12]

Waters and King considered the case of a viscoelastic liquid of integral type, and for the Oldroyd fluids in particular. Their solution, expressed again in terms of Fourier–Bessel series, shows that, for sufficiently large values of the elastic parameters, the velocity profiles may overshoot the asymptotic velocity and oscillate around it for quite a long time.[32]

Balmer and Fiorina described the impulsively started flow of a power-law fluid, and obtained a variety of solutions as the power index varies.[2]

An impulsive flow of a dusty (two phases) fluid through a circular pipe induced by an impulsive pressure gradient is considered in Ref. 10.

In Ref. 17, the starting and stopping flows of a biviscosity fluid through a pipe with and without stenosis are considered. The start-up flow of an Oldroyd-B fluid between two rotating concentric cylinders is studied in Ref. 11: an overshooting of the dynamical variables is observed and a comparison with measurements in experiments is given.

More recently, an analytical solution in the case of upper-convected Maxwell fluid is derived in several cases of pressure gradient[24] and solutions are extended for tubes of rectangular cross-section.[25]

Other mathematical models for unsteady pipe flows with pressure gradients of different types have been developed and solved analytically or numerically, and reveal a great effort in describing or predicting important effects in biological flows or in processing operations.[1,26]

A relevant example of a non-Newtonian liquid is the blood. Blood is a suspension of different cells in the plasma: among these, the red cells have a dominant influence in hemodynamics: although plasma is constituted by 90% water and can be considered a Newtonian fluid, it is commonly assumed that blood is a non-Newtonian fluid, because the elastic and deformable structure of red cells gives it a shear dependent viscosity and a viscoelastic nature.[8,11,14,16,22]

Due to its complex chemical structure, a theoretical universal reliable model for blood in the mechanics of continuum is still lacking. Although it has been well established that blood is both a viscoelastic and a shear-thinning liquid, the connection of these two aspects has not yet been clarified.

However, many mathematical models for describing rheological behavior of blood have been extensively developed in the last decades[8,16,19,29,31] (see Ref. 27 for a recent review).

Due to the high nonlinear behavior of these non-Newtonian models, some appropriate simplification in the flow is necessary. The first step in understanding mechanics of circulation is the investigation of the flows in straight uniform tubes: any spurious effect due to the geometry is removed.

Although a lot of work has been carried out in steady flows, only few studies in unsteady flows are available. Actually, the blood circulation system gives rise to regions where the fluid is significantly accelerated and therefore to changing flow rates.

Moreover, there is some evidence that many hemodynamical anomalies are related to transient flows, and the alteration of the shear stress at the wall is related to the sudden variation of some physical variables.[6,15,18] Therefore, it becomes extremely important to analyze transient regimes.

The purpose of this work is to describe a new generalized Oldroyd-B model, used mainly for blood or for similar biological fluids.[34] It includes a shear rate dependent viscosity and has been proved effective in many fluid flows. The model is first presented in Ref. 35, where a range of values of the material constants is determined. Starting from those issues, the behavior of such a model in 1-D flow in a tube of infinite length and circular cross-section, driven by an oscillatory pressure gradient was studied in Ref. 23. The combined effect of the viscoelasticity and of the shear rate dependent viscosity was pointed out.

Here the flow driven by an impulsive pressure gradient is considered. Although this flow appears to be unrealistic to describe the real blood circulation, nevertheless, it offers a useful tool for setting up the model and for understanding the main characteristic of the unsteady flows, since any pressure pulse can be regarded as a superposition of a step function with a train of oscillations of the pressure gradient.[17,18]

The coupled constitutive and motion equations form a nonlinear system which is solved numerically. We used a spectral method with collocation in space and a finite difference method in time.

The flow dependence on the dimensionless parameters in connection with the unsteadiness is investigated carefully. The numerical results have been compared first with the analytical solution available in some particular cases, and then with other numerical studies in literature.

2. The Generalized Oldroyd-B Model

The inadequacy of the classical Navier–Stokes theory in describing rheological complex fluids such as blood, paints, oils, polymeric solutions, led to the development of several theories in the field of the non-Newtonian fluid mechanics.

Since a time lag in the response of the fluid to changes in applied forces is observed, rate type models are commonly used to describe such strain and stress history dependence.

In the classical Oldroyd-B model,[20] the relationship between the extra-stress tensor $\mathbf{S}$ and the stretching tensor $\mathbf{A}_1$ is given by:

$$\mathbf{S} + \lambda_1(\dot{\mathbf{S}} - \mathbf{LS} - \mathbf{SL}^{\mathrm{T}}) = \mu[\mathbf{A}_1 + \lambda_2(\dot{\mathbf{A}}_1 - \mathbf{LA}_1 - \mathbf{A}_1\mathbf{L}^{\mathrm{T}})]\,, \tag{2.1}$$

where

$$\mathbf{A}_1 = (\mathrm{grad}\ \mathbf{v}) + (\mathrm{grad}\ \mathbf{v})^{\mathrm{T}}$$

μ is a constant viscosity, λ_1 and λ_2 are two constants having the dimension of time ($\lambda_1 > \lambda_2 \geq 0$), referred to as relaxation and retardation time respectively.[a] Their effect is to include into the model two well-known phenomena in unsteady flows of many fluids: stress relaxation and the creep.[4,14] This model combines a relative simplicity with the ability to predict other properties of some fluid at relatively low shear rate, such as the normal stress. Actually, experimental results show that, mostly in unsteady flows, many fluids are not purely viscous, but show significant viscoelastic properties.[8,11,22]

Results of simulations are of qualitative interest, and at low flow rate, they also have quantitative significance.

On the other hand, many inelastic models exist in literature and are able to describe shear-thinning fluids through a functional dependence of μ from $\dot{\gamma}$.[2,14] The function $\mu(\dot{\gamma})$, which depends on the specific fluid, can be replaced instead of the constant viscosity μ in (2.1). Thus, the Oldroyd-B model can be easily generalized with the use of a nonconstant viscosity as follows:

$$\mathbf{S} + \lambda_1(\dot{\mathbf{S}} - \mathbf{LS} - \mathbf{SL}^{\mathrm{T}}) = \mu(\dot{\gamma})\mathbf{A}_1 + \eta_0\lambda_2(\dot{\mathbf{A}}_1 - \mathbf{LA}_1 - \mathbf{A}_1\mathbf{L}^{\mathrm{T}}) \tag{2.2}$$

with η_0 a constant with the dimension of a viscosity (see Sec. 3).

It can be verified that the model (2.2), as (2.1), satisfies the principle of material frame invariance.[35]

Equation (2.2), by combining elastic and viscous terms, can be used to predict, at least qualitatively, many of the properties observed in viscoelastic fluids. Actually, the use of a nonconstant viscosity $\mu(\dot{\gamma})$ in (2.2) allows the model to be representative of a larger class of fluids which possess a marked shear rate dependence of viscosity.

The model (2.2) reduces to a pure inelastic fluid when $\lambda_1 = \lambda_2 = 0$ and to the Navier–Stokes linear model when, in addition, $\mu(\dot{\gamma}) = \mathrm{const}$.

3. The Viscosity of Blood

Let us now confine our attention to the most important biological fluid: the blood. While the linear theory of Navier–Stokes fluid is acceptable for modeling blood flow in large arteries, the role of material nonlinearity and the effect of red blood cells on the viscosity, becomes more important at low shear rates ($< 100\ \mathrm{s}^{-1}$) as well as in smaller vessels, where flows cannot be well described by a simplicistic linear constitutive equation.[7]

[a]The dot above a variable f (scalar, vector or tensor) denotes the material derivative as in: $\dot{f} = \frac{\partial f}{\partial t} + \mathbf{v} \cdot \mathrm{grad}\ f$.

In the microcirculation, both the Reynolds and Womersley numbers are small because of the small size of the vessels and the low flow velocities. Moreover, near the center of the large vessels, or in separated regions of recirculating flow, the average value of shear rate will be small. Furthermore, in unsteady flows, the wall shear stress may be, in some instants, considerably small.

In all these cases, the viscosity cannot be considered as a constant, but as a decreasing function of the rate of shear $\dot{\gamma}$. In the last years, many functions have been proposed to model the nonlinear dependence of the viscosity of the blood on the strain rate.[8,16,19] Due to the variable behavior and the complex chemical structure of this liquid, none of the models seem to be completely satisfactory for all kinds of flow regimes.

Experimental evidence shows that, while the plasma is a fluid with no significant departure from Newtonian behavior, when red blood cells are present in plasma, the viscosity of the whole mixture increases considerably at low shear rate (*shear-thinning* fluid).[7] Actually, the blood cells tend to move as rigid particles when the shear stress is small and not sufficient to deform them very much. As a consequence, they tend to produce a higher apparent viscosity. At a large shear rate, the stresses are sufficient to deform the cells extensively, so that they contribute in a smaller dissipation of energy, and hence the apparent viscosity is lower.

General regression analysis of experimental data suggests the use of some complicated transcendental functions for $\mu(\dot{\gamma})$. Since the apparent viscosity has two distinct asymptotic values η_0 and η_∞ as $\dot{\gamma} \to 0$ and ∞ respectively ($\eta_0 \geq \eta_\infty$), the analytical function which offers the best fit of experimental data for a quite large range of flows has been found to be:

$$\mu(\dot{\gamma}) = \eta_\infty + (\eta_0 - \eta_\infty)\left[\frac{1+\log(1+\Lambda\dot{\gamma})}{1+\Lambda\dot{\gamma}}\right], \quad \dot{\gamma} = \left[\frac{1}{2}\mathrm{tr}(\mathbf{A}_1^2)\right]^{1/2}, \tag{3.3}$$

with $\Lambda \geq 0$ a material constant with the dimension of time representing the degree of shear-thinning[34,35] (for $\Lambda = 0$ or for $\eta_0 = \eta_\infty$ a constant viscosity is obtained). The complex viscosity of blood is approximated here with a three-parameter model, where the apparent viscosity decreases dramatically as the rate of shear increases (see Fig. 1). The asymptotic values η_0 and η_∞ are present in many other inelastic shear-thinning models and their values have set up through experiments (see Sec. 6).[19]

Although a pure inelastic model based on (3.3) catches some aspects of the shear-thinning, but does not address any shear history dependence, it is insufficient to correctly describe the unsteady blood flow. A more comprehensive model for blood is given by incorporating the expression of the viscosity (3.3) in the viscoelastic model (2.2).

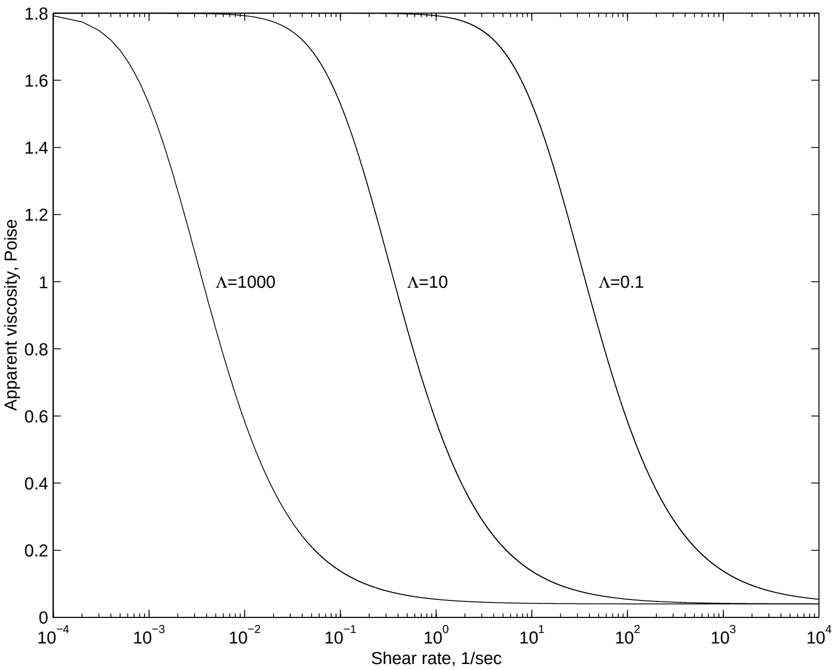

Fig. 1. The shear rate dependent viscosity function (3.3) with $\eta_0 = 180$ cP, $\eta_\infty = 4$ cP for three values of Λ (in sec).

4. Formulation of the Problem

Let us consider a fluid of constitutive Eqs. (2.2) and (3.3) flowing in a straight long pipe of circular cross-section having radius R.[b]

The fluid is assumed to be an isotropic, homogeneous and incompressible continuum of constant density ρ, and the vessel walls are considered rigid and impermeable.

The motion equation is:

$$\rho\frac{\partial \mathbf{v}}{\partial t} + \mathbf{v}\cdot\nabla\mathbf{v} = \mathrm{div}\ \mathbf{T}\,, \qquad \mathbf{T} = -p\mathbf{I} + \mathbf{S}\,, \tag{4.4}$$

where $\mathbf{v} = (u, v, w)$ is the velocity vector and the external forces are assumed to be negligible.

Let us now consider a cylindrical coordinate system (r, θ, z) having the z-axis coincident with the pipe axis. In the hypothesis of laminar flow, the only nonzero component of velocity is w. Moreover, since the flow is assumed to be axisymmetric and with no entry effect, the fluid dynamical variables do depend on r and t only, except for the pressure which depends on z and t only. In such hypothesis the convective term in (4.4) vanishes.

[b]Here *long* means of length much larger than the radius of the pipe.

We are interested in two opposite step changes in pressure gradient taking place as follows:

(a) the fluid, initially at rest, is set in motion at $t = 0$ by a constant pressure gradient C imposed suddenly and maintained in time (*starting or start-up* (SU) *flow*), i.e.

$$\frac{dp}{dz} = \begin{cases} 0 & t \le 0\,, \\ C & t > 0\,. \end{cases} \tag{4.5}$$

(b) A fully developed Poiseuille flow is initially driven by a constant pressure gradient C which is suddenly removed at time $t = t^*$ (*stopping or shut-down* (SD) *flow*), i.e.

$$\frac{dp}{dz} = \begin{cases} C & t \le t^*\,, \\ 0 & t > t^*\,. \end{cases} \tag{4.6}$$

The constitutive equation (2.2), with the expression of viscosity (3.3) coupled with the motion equation (4.4), gives:

$$\begin{aligned} &\rho\,\frac{\partial w}{\partial t} = -\frac{dp}{dz} + \frac{\partial S_{rz}}{\partial r} + \frac{S_{rz}}{r}\,, \\ &S_{rz} + \lambda_1 \frac{\partial S_{rz}}{\partial t} = \left[\eta_\infty + (\eta_0 - \eta_\infty)\frac{1 + \log\sigma}{\sigma}\right]\frac{\partial w}{\partial r} + \eta_0\lambda_2 \frac{\partial^2 w}{\partial r \partial t}\,, \\ &S_{zz} + \lambda_1\left(\frac{\partial S_{zz}}{\partial t} - 2\frac{\partial w}{\partial r}S_{rz}\right) = -2\eta_0\lambda_2\left(\frac{\partial w}{\partial r}\right)^2\,, \end{aligned} \tag{4.7}$$

where

$$\sigma = 1 + \Lambda\left|\frac{\partial w}{\partial r}\right|\,.$$

The boundary conditions associated to the physical problem are given by:

$$w = 0 \quad \text{at } r = R \tag{4.8}$$

(no slip velocity at the wall) and

$$\frac{dw}{dr} = 0 \quad \text{at } r = 0 \tag{4.9}$$

(axisymmetry). For the SU flow (4.5), a zero velocity field is considered as initial condition. Then, the flow develops at some steady state time t^*, and the fully developed flow pattern is used as initial condition for the SD flow (4.6).

By introducing the following change of variables:

$$r \to \frac{r}{R}\,, \qquad z \to \frac{z}{R}\,, \qquad t \to \frac{Wt}{R}\,,$$

$$p \to \frac{p}{\rho W^2}\,, \qquad w \to \frac{w}{W}\,, \qquad S_{rz} \to \frac{S_{rz}}{\rho W^2}\,, \qquad S_{zz} \to \frac{S_{zz}}{\rho W^2}$$

with W a characteristic velocity and by redefining the following dimensionless constants:

$$Re = \frac{RW}{\nu}, \quad \gamma = \frac{\eta_\infty}{\eta_0}, \quad C \to \frac{CR}{\rho W^2}, \quad T \to \frac{TW}{R},$$

$$\lambda_1 \to \frac{\lambda_1 W}{R}, \quad \lambda_2 \to \frac{\lambda_2 W}{R}, \quad \Lambda \to \frac{\Lambda W}{R}$$

with $\nu = \eta_0/\rho$ a kinematic viscosity, the system (4.7) is nondimensionalized as:

$$\begin{aligned} &\frac{\partial w}{\partial t} = -\frac{\partial p}{\partial z} + \frac{\partial S_{rz}}{\partial r} + \frac{S_{rz}}{r}, \\ &S_{rz} + \lambda_1 \frac{\partial S_{rz}}{\partial t} = \frac{1}{Re}\left\{\left[\gamma + (1-\gamma)\frac{1+\log\delta}{\delta}\right]\frac{\partial w}{\partial r} + \lambda_2 \frac{\partial^2 w}{\partial r \partial t}\right\}, \\ &S_{zz} + \lambda_1\left(\frac{\partial S_{zz}}{\partial t} - 2\frac{\partial w}{\partial r} S_{rz}\right) = -2\frac{\lambda_2}{Re}\left(\frac{\partial w}{\partial r}\right)^2, \end{aligned} \tag{4.10}$$

equations to be solved for $0 \le r \le 1$ where

$$\delta = 1 + \Lambda \left|\frac{\partial w}{\partial r}\right| .$$

Note that (4.10.1) and (4.10.2) constitute a nonlinear autonomous subsystem. Equation (4.10.3) has no spatial derivative in S_{zz} and the solution can be easily found once the values of w and S_{rz} are known.

4.1. *Special cases*

When the parameters attain special values, some simplification of the problem is possible, because one or more terms in the system (4.10) disappear.

For example, for $\gamma = 1$ an analytical solution for the Oldroyd fluids can be easily recovered as in Ref. 12.

In the case of the Maxwell fluid ($\gamma = 1, \lambda_2 = 0$), combination of (4.10.1) and (4.10.2) leads to the following linear equation in w:

$$\lambda_1 \frac{\partial^2 w}{\partial t^2} + \frac{\partial w}{\partial t} - \frac{1}{Re}\left(\frac{\partial^2 w}{\partial r^2} + \frac{1}{r}\frac{\partial w}{\partial r}\right) = -\frac{\partial p}{\partial z} - \lambda_1 \frac{\partial^2 p}{\partial z \partial t}$$

and this can be easily solved by separation of variables, expressing the solution with Bessel functions.[24]

In particular, the Newtonian case is recovered when, in addition, $\lambda_1 = 0$. In such a case, the system (4.10) reduces immediately to just one first-order equation.[3,28]

Finally, for $\lambda_1 = \lambda_2 = 0$, we have:

$$S_{rz} = \frac{1}{Re}\left[\gamma + (1-\gamma)\frac{1+\log\delta}{\delta}\right]\frac{\partial w}{\partial r}, \quad S_{zz} = 0 . \tag{4.11}$$

5. Numerical Method

The complexity of the non-Newtonian flows requires accurate and efficient numerical techniques, due to the nonlinear nature of the governing equations. The system (4.10.1) and (4.10.2) is rewritten as:

$$\frac{\partial \phi}{\partial t} = L(\phi) + f(t)\,, \tag{5.12}$$

where $\phi = (w, S_{rz})$ and L is the nonlinear differential operator for spatial terms and f is the forcing term. Then, the P.D.E. (5.12) is split into two subsequent differential problems consisting first in discretizing the spatial operator L with an accurate and efficient method, and in integrating a system of O.D.E.'s in time with a low order finite difference scheme.[5,33] Due to the stronger dependence on the space variables, the higher order and the nonlinearities, a spectral collocation method has been used to discretize the spatial operator L.[5,13,21,33]

The unknown function ϕ is approximated by a truncated series of polynomials $p_j \in \mathbf{P}_n$, where $\mathbf{P}_n$ is the space of polynomials of degree $\leq n$:

$$\phi \approx p = \sum_{j=0}^{n} c_j p_j\,.$$

Let us denote with $\eta_i, 1 \leq i \leq n-1$ the zeros of the derivative of the orthogonal Legendre polynomial of degree n in $[-1, 1]$, being $\eta_0 = -1, \eta_n = 1$ the extrema points (Legendre Gauss–Lobatto points). If a representation for p is used in the physical space (canonical Lagrange basis with respect to the set of $(\eta_i)_{i=0,\ldots,n}$), we have:

$$p(x) = \sum_{j=0}^{n} p(\eta_j) l_j(x)\,, \tag{5.13}$$

where the basis (l_j) is such that:

$$l_j(\eta_i) = \delta_{ji}\,.$$

Expressions for derivatives with respect to the same basis are easily obtainable by replacing coefficients in (5.13) with other tabulated values.[13]

Equation (5.12) is then replaced by rescaling the operator L in $[-1, 1]$ and by collocating ϕ at $(\eta_i)_{i=0,\ldots,n}$, i.e.

$$\frac{\partial \phi}{\partial t}(\eta_i) = L(\phi)(\eta_i) + f(t)\,, \quad i = 0, \ldots, n$$

and boundary conditions are imposed at η_0 and η_n.

Once an approximated solution is written as (5.13), the problem is reduced to solving the system of first order O.D.E.'s:

$$\frac{d\phi_i}{dt} = L(\phi_i(t)) + f(t) \quad \text{with } \phi_i = \phi(\eta_i)\,, \quad i = 0, \ldots, n\,. \tag{5.14}$$

We choose the implicit finite trapezoidal scheme for solving the system (5.14):

$$\phi_i^{k+1} - \phi_i^k = \frac{\Delta t}{2}[L(\phi_i^k) + L(\phi_i^{k+1})] + f^{k+1}\,, \quad i = 0, \ldots, n \tag{5.15}$$

where the new solution is computed at time $t = (k+1)\,\Delta t$. It has been proved that it is unconditionally stable and second order accurate.[5]

Being L a nonlinear operator, we solve (5.15) by linearized iterations at each time step, computing the viscosity coefficient $[\gamma + (1-\gamma)\frac{1+\log\delta}{\delta}]$ explicitly. The iteration proceeds until convergence is reached.[9] Such linearization of L is devised in such a way that only the terms corresponding to the Laplacian operator L_Δ have been discretized implicitly so that the problem (5.14) is well posed.[5]

Then, a value for S_{zz} is obtained explicitly by discretizing Eq. (4.10.3).

The coefficients $p(\eta_i)$ in (5.13) are then computed at each time step as a solution of the algebraic linear system of order $n+1$:

$$\left(I - \frac{\Delta t}{2}L_\Delta\right)\phi_i^{k+1} = \left(I + \frac{\Delta t}{2}L\right)\phi_i^k + f^{k+1}\,, \quad i = 0, \ldots, n\,.$$

This is the major time-consuming step in the integration procedure, because of the iteration loop within each time step: the system has been solved by a LU factorization of the matrix of the coefficients with partial pivoting (routine F04AAF — NAG Library). Other more efficient ways to solve it are worth being investigated.

Note that the same set of collocation points (η_i) is chosen at each time step and the solution is computed by interpolation over a set of equidistributed points.

6. Results and Discussion

Nonlinear models turn out to be very sensitive to the choice of the material parameters which characterize the specific flow problem. Since we restrict ourselves to the flow in small vessels, the following parameters have been fixed, being of interest in a physiological context[18]:

$$Re = 0.1\,, \quad \gamma = 0.022\,, \quad C = 1$$

and the others are varied in a typical range to test the sensitivity of the system to their perturbation.

Simulations have been carried out with $\Delta t = 10^{-4}$ and the spectral method is implemented over $n = 20$ collocation points.

The numerical solution obtained setting $\lambda_1 = \lambda_2 = \Lambda = 0$ is compared with the exact solution in the case of Navier–Stokes fluid, to give some estimate on the accuracy and stability of the numerical method.[3] The fine agreement obtained ($\|e\|_\infty \leq 1.E^{-5}$) confirms the effectiveness of the scheme used.

To evaluate the importance of the concurrent viscous and elastic forces and in order to understand the role of each of them in SU and SD flows, two other simple cases are analyzed:

(a) $\lambda_1 = \lambda_2 = 0$ (pure shear-thinning fluid) and

(b) $\Lambda = 0$ (Oldroyd-B fluid).

The full model is used when:

(c) $\lambda_1 \neq 0, \lambda_2 \neq 0, \Lambda \neq 0$ (Generalized Oldroyd-B fluid).

Computation of hemodynamical variables is of much importance in the localization of vascular diseases or in clinical procedures, such as remodeling vascular wall or design of artificial prostheses.

For example, the magnitude and the variation of the wall shear stress (WSS) are relevant clues for the localization and prediction of diseases in blood vessels.[6] Unfortunately, WSS is not easily measurable in unsteady flows.

The centerline velocity (CV) is a representative measure of the inertia of the fluid, while the flow rate, computed as:

$$Q = 2\pi \int_0^1 wr\,dr$$

is an estimate of the magnitude of the flow and provides an important average information. No significant difference is found in the evolution of CV and Q.

In case (a), CV increases monotonically up to the steady state value. The asymptotic value reached at steady state time increases with Λ for CV, confirming the results in Ref. 23, but does not change for WSS, which is the value of the Poiseuille flow (WSS $\to C/2$). In transient regimes, the larger Λ is, the smaller the value of instantaneous WSS for SU flow, the larger for SD flow.

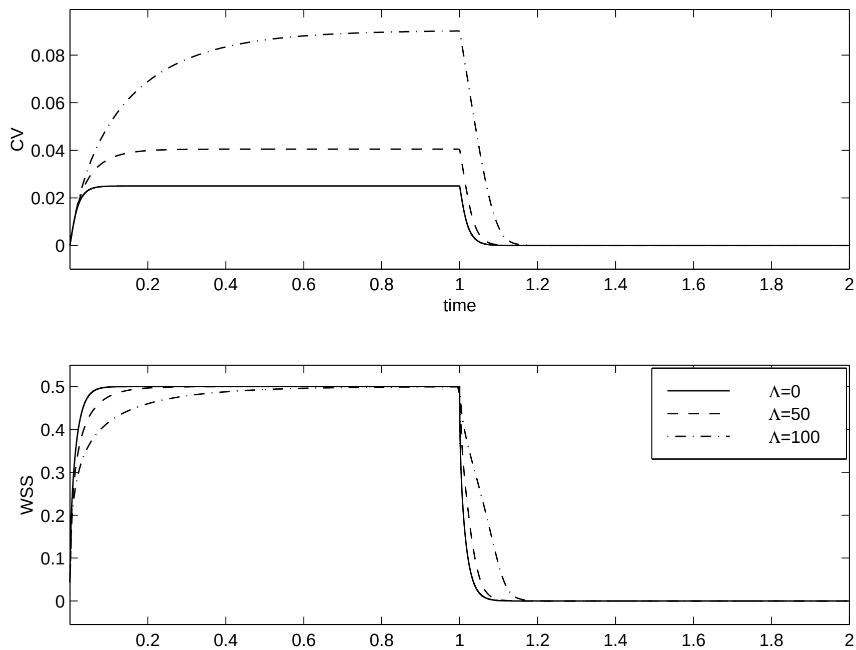

Fig. 2. Time histories for CV and WSS in SU and SD flows. Case (a).

The transient time for SD flow is much shorter than for SU (see Fig. 2).

In case (b), the transient regimes are characterized by initial overshooting followed by damped oscillations towards a steady state value which is the same as in the Newtonian case, for all variables (CV $\to Re\, C/4$; WSS $\to C/2$). This phenomenon, due do the elasticity in the fluid and confirmed by the experiments, was already observed and discussed in Refs. 11, 12 and 32.

The amplitude of this pulse grows with the ratio λ_1/λ_2 (it can reach 400% of the terminal value for CV, less for WSS), and its damping strengthens at larger λ_2. These results are in accordance with those in Ref. 34, where a first analysis has been developed and a comparison with real data coming from measurements has been carried out. Note that the peaks of CV are attained at times different from those of WSS (Fig. 3).

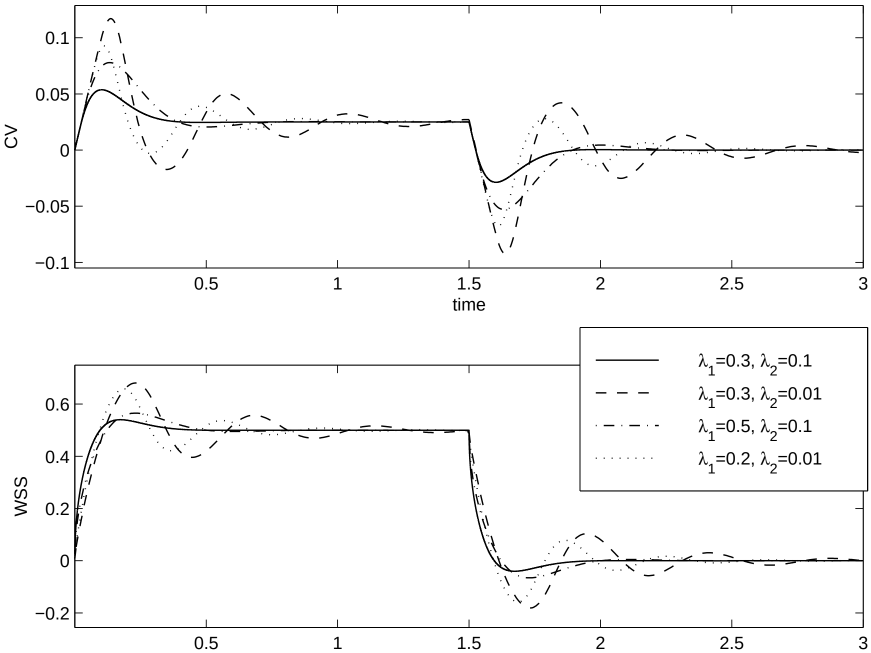

Fig. 3. Time histories for CV and WSS in SU and SD flows. Case (b).

In both (a) and (b) the steady state time is larger than in Navier–Stokes case.

When the complete model (c) is used, a combination of the effects present in (a) and (b) is observed. The amplitude of oscillations about the terminal value can be smaller or larger depending on the size of $\lambda_1, \lambda_2, \Lambda$. These oscillations are reduced in number or disappear (see Fig. 4). The final value of CV rises with Λ, while no effect of Λ is reported on the terminal value of WSS.

As in (a) the SD process is faster than that of the SU, and the symmetry between the SU and SD cases is lost.

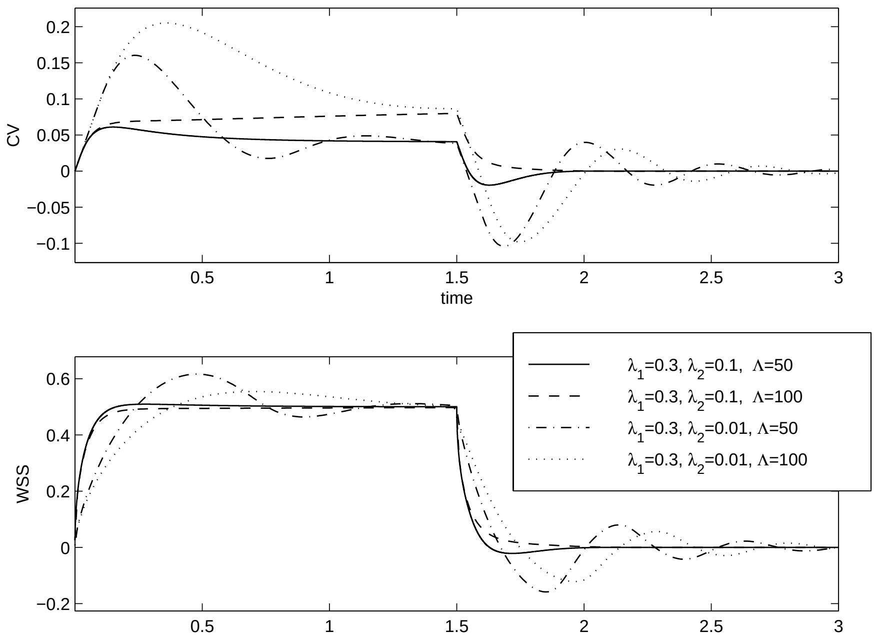

Fig. 4. Time histories for CV and WSS in SU and SD flows. Case (c).

Other physical phenomena have some clinical implications: as expected, the velocity near the wall exhibits smoother oscillations than CV, due to the fact that the viscosity is confined to a narrow layer near the wall. As a consequence, the effect of unsteadiness is more evident at the center, because this region responds more promptly to variations in the driving pressure gradient. Phenomena of backflow can be present (Fig. 5).

While in case (a) $S_{zz} = 0$ (cf. (4.11)), in the other cases the normal stress S_{zz} is not zero, being greatly enhanced in case (c) and showing characteristics of a plug flow (Fig. 6).

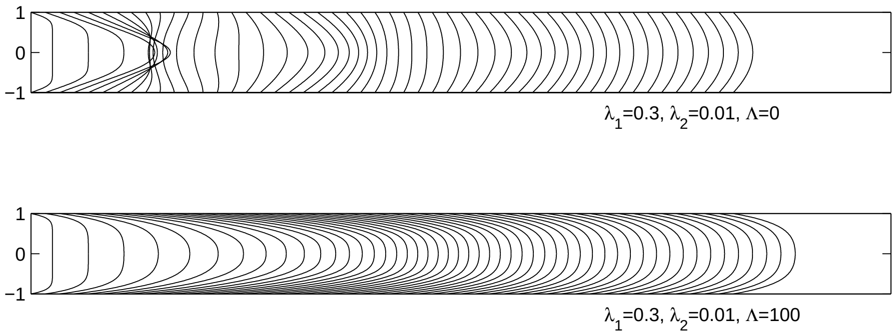

Fig. 5. Velocity profiles shifted in time in SU flow. Comparison between cases (b) and (c).

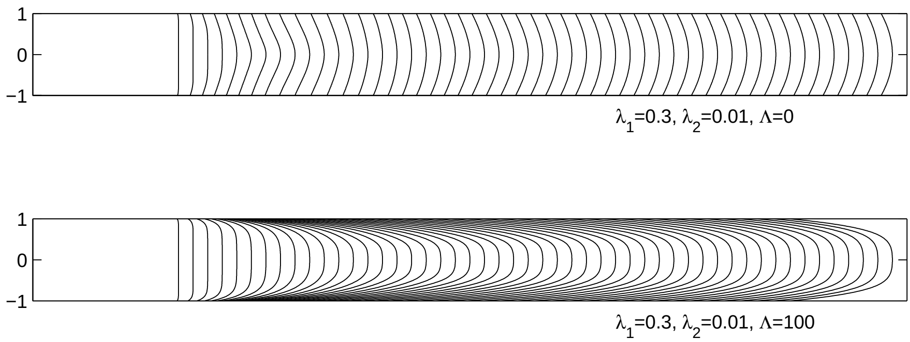

Fig. 6. S_{zz} profiles shifted in time in SU flow. Comparison between cases (b) and (c).

It is worth noting that differences with the Newtonian case are emphasized for a smaller Re.

7. Conclusions

Computational biofluid mechanics play an important role in the understanding of the development and the progression of vascular pathologies.

Though the detailed knowledge of the dynamical variables is possible and provides useful elements, the mechanism of influence of the hemodynamical factors in the arterial diseases is not yet clear.

In large vessels, the specific nature of the blood may be ignored and, as a consequence, it can be considered as an incompressible Newtonian fluid. In smaller vessels, the inertial terms become negligible, but the nature of the red blood cells must be taken into consideration, by including a shear-rate dependent viscosity in the diffusion terms.

Blood circulation is dominated by unsteady flow phenomena. It is found that a pure inelastic model is not representive of the rheological behavior of blood, since the role of viscoelasticity becomes important in time-dependent flows.

We presented both a viscoelastic and shear-thinning continuum model able to describe a pipe flow even from a quantitative point of view. The formulation of such a model is derived from the elastic properties and the structure of the red blood cells. Also the distribution and the interaction of cellular constituents is an important factor to assess the fundamental rheological properties of the blood.

A preliminary study on the impulsive flow in a straight arterial segment has been carried out, under the assumption of rigid vessel walls. The vessel diameter change is approximately 5–10% in most of the major arteries, smaller in capillaries and, as a first approximation, this hypothesis is acceptable, in the limit of small Reynolds numbers.

This work offers a basis for a better understanding of blood flow unsteady phenomena in small arteries, constitutes a necessary first step in the development of the computational framework, and gives some hints on the mechanical forces and physical phenomena occurring in more complex flows.

The results presented show that a combination between a viscoelastic and a shear-thinning fluid induces effects which may not be present in each of them alone. According to the mutual size of the parameters, one may be dominant or may enhance the other one. The most evident are the overshooting of the dynamical variables and the increased magnitude of their terminal values.

All these fluid mechanical aspects are revealed as extreme importance in blood flow and need to be further refined. The important mechanism of the diffusion of the viscosity has to be explored in other realistic geometries. A great deal of work will be devoted to understand the connection and the influence of such aspects with the biological and clinical facts.

Acknowledgment

This work has been partially supported by the *Progetto Strategico: Metodi e Modelli Matematici nello studio di fenomeni biologici* of CNR, Italy.

References

1. H. I. Andersson and K. L. Tiseth, *Start-up flow in a pipe following the sudden imposition of a constant flow rate, Chem. Eng. Comm.* **11** (1992) 121–133.
2. R. T. Balmer and M. A. Fiorina, *Unsteady flow of an inelastic power-law fluid in a circular tube, J. Non-Newtonian Fluid Mech.* **7** (1980) 189–198.
3. G. K. Batchelor, **An Introduction to Fluid Dynamics** (Cambridge Univ. Press, 1967).
4. R. B. Bird, R. C. Armstrong and O. Hassager, **Dynamics of Polymeric Liquids, Vol. 1: Fluid Mechanics** (John Wiley & Sons, 1987).
5. C. Canuto, M. Y. Hussaini, A. Quarteroni and T. A. Zang, **Spectral Method in Fluid Dynamics** (Springer-Verlag, 1987).
6. C. G. Caro, T. J. Pedley, R. C. Schroter and W. A. Seed, **The Mechanics of the Circulation** (Oxford University Press, 1978).
7. S. Chien, S. Usami and R. Skalak, *Blood flow in small tubes*, in **American Physiology Society Handbook of Physiology** (American Physiology Society, 1984), Vol. 4, Sec. 2, pp. 217–249.
8. H. Chmiel, I. Anadere and E. Walitza, *The determination of blood viscoelasticity in clinical hemorheology, Biorheology* **27** (1990) 883–894.
9. R. Courant and D. Hilbert, **Methods of Mathematical Physics** (Interscience, 1962), Vol. II.
10. N. Datta and D. C. Dalal, *Unsteady flow of a dusty fluid through a circular pipe with impulsive pressure gradient, Acta Mech.* **95** (1992) 51–57.
11. S. Deutsch, W. M. Phillips and J. Heist, *An interpretation of low strain rate blood viscosity measurements: a continuum approach, Biorheology* **13** (1976) 297–307.
12. I. Etter and W. R. Schowalter, *Unsteady flow of an Oldroyd fluid in a circular tube, Trans. Soc. Rheol.* **9** (1965) 351–369.
13. D. Funaro, **Polynomial Approximation of Differential Equations** (Springer-Verlag, 1992).
14. Y. C. Fung, **Biodynamics: Circulation** (Springer-Verlag, 1984).

15. D. N. Ku, *Blood flow in arteries, Ann. Rev. Fluid Mech.* **29** (1997) 399–434.
16. D. E. Mann and J. M. Tarbell, *Flow of non-Newtonian blood analog fluids in rigid curved and straight artery models, Biorheology* **27** (1990) 711–733.
17. M. Nakamura and T. Sawada, *Numerical study of the unsteady flow of non-Newtonian fluid, ASME J. Biomech. Engg.* **112** (1992) 100–103.
18. W. W. Nichols and M. F. O'Rourke, **McDonald's Blood Flow in Arteries** (Edward Arnold, 1990).
19. C. Oiknine, *Rheology of the human blood*, in **Adv. Cardiovasc. Phys.**, Karger, Basel (1983), Part I, Vol. 5, pp. 1–25.
20. J. G. Oldroyd, *On the formulation of rheological equations of state, Proc. R. Soc. London A* **200** (1950) 523–541.
21. T. N. Phillips, *On the potential of spectral methods to solve problems in non-Newtonian fluid mechanics, Num. Methods Part. Differential Equation* **5** (1989) 35–43.
22. W. M. Phillips and S. Deutsch, *Toward a constitutive equation for blood, Biorheology* **12** (1975) 383–389.
23. G. Pontrelli, *Pulsatile blood flow in a pipe, Comput. Fluids* **27** (1998) 367–380.
24. K. D. Rahaman and H. Ramkissoon, *Unsteady axial viscoelastic pipe flows, J. Non-Newtonian Fluid Mech.* **57** (1995) 27–38,.
25. H. Ramkissoon, C. V. Easwaran and S. R. Majumdar, *Unsteady flow of an elastico-viscous fluid in tubes of uniform cross-section, Internat. J. Nonlinear Mech.* **24** (1989) 585–597.
26. J. N. Reddy and V. A. Padhye, *A penalty finite element model for axisymmetric flows of non-Newtonian fluids, Num. Methods Part. Differential Equation* **4** (1988) 33–56.
27. R. Skalak, N. Özkaya and T. C. Skalak, *Biofluid mechanics, Ann. Rev. Fluid Mech.* **21** (1989) 167–204.
28. P. Szymanski, *Quelques solutions exactes des équations de l'hydrodynamique du fluide visqueux dans le cas d'un tube cylindrique, J. Math. Pure Appl. Ser.* **11** (1932) 67–107.
29. G. B. Thurston, *Effect of viscoelasticity of blood on wave propagation in the circulation, J. Biomech.* **9** (1976) 13–20.
30. T. W. Ting, *Certain non-steady flows of second-order fluids, Arch. Rat. Mech. Anal.* **14** (1964) 1–26.
31. F. J. Walburn and D. J. Schneck, *A constitutive equation for whole human blood, Biorheology* **13** (1976) 201–210.
32. N. D. Waters and M. J. King, *The unsteady flow of an elastico-viscous liquid in a straight pipe of circular cross-section, J. Phys.* **D4** (1971) 204–211.
33. S. Xu, A. R. Davies and T. N. Phillips, *Pseudospectral method for transient viscoelastic flow in an axisymmetric channel, Num. Methods Part. Differential Equation* **9** (1993) 691–710.
34. K. K. Yeleswarapu, *Evaluation of continuum models for characterizing the constitutive behavior of blood*, Ph.D. Thesis, University of Pittsburgh (1996).
35. K. K. Yeleswarapu, J. F. Antaki, H. Borovetz and K. R. Rajagopal, *The flow of blood in tubes: theory and experiments*, to appear in *Mech. Res. Comm.*

This article has been cited by:

1. A. M. SIDDIQUI, T. HAROON, Z. BANO, S. ISLAM. 2013. PRESSURE FLOW OF A SECOND GRADE FLUID THROUGH A CHANNEL OF VARYING WIDTH WITH APPLICATION TO STENOSED ARTERY. *International Journal of Biomathematics* **06**:03. . [Abstract] [PDF] [PDF Plus]
2. Antonio Fasano, Angiolo Farina. 2012. Modeling high flux hollow fibers dialyzers. *Discrete and Continuous Dynamical Systems - Series B* **17**:6, 1903-1937. [CrossRef]
3. GUL ZAMAN, YONG HAN KANG, IL HYO JUNG. 2011. ORIENTATIONAL STRESS TENSOR OF POLYMER SOLUTION WITH APPLICATIONS TO BLOOD FLOW. *Modern Physics Letters B* **25**:12n13, 1157-1166. [Abstract] [References] [PDF] [PDF Plus]
4. S. SEN, S. CHAKRAVARTY. 2007. A NONLINEAR UNSTEADY RESPONSE OF NON-NEWTONIAN BLOOD FLOW PAST AN OVERLAPPING ARTERIAL CONSTRICTION. *Journal of Mechanics in Medicine and Biology* **07**:04, 463-489. [Abstract] [References] [PDF] [PDF Plus]